



**HAL**  
open science

# In vitro digestion of complex foods: How microstructure influences food disintegration and micronutrient bioaccessibility

Manon Hiolle, Valérie Lechevalier-Datin, Juliane Floury, Nathalie N. Boulier-Monthéan, C. Prioul

## ► To cite this version:

Manon Hiolle, Valérie Lechevalier-Datin, Juliane Floury, Nathalie N. Boulier-Monthéan, C. Prioul. In vitro digestion of complex foods: How microstructure influences food disintegration and micronutrient bioaccessibility. Food Research International, 2020, 128, pp.108817. 10.1016/j.foodres.2019.108817. hal-02485321

**HAL Id: hal-02485321**

<https://institut-agro-rennes-angers.hal.science/hal-02485321>

Submitted on 21 Jul 2022

**HAL** is a multi-disciplinary open access archive for the deposit and dissemination of scientific research documents, whether they are published or not. The documents may come from teaching and research institutions in France or abroad, or from public or private research centers.

L'archive ouverte pluridisciplinaire **HAL**, est destinée au dépôt et à la diffusion de documents scientifiques de niveau recherche, publiés ou non, émanant des établissements d'enseignement et de recherche français ou étrangers, des laboratoires publics ou privés.



Distributed under a Creative Commons Attribution - NonCommercial 4.0 International License

## ***In vitro* digestion of complex foods: How microstructure influences food disintegration and micronutrient bioaccessibility**

Hiolle M.<sup>a</sup>, Lechevalier V.<sup>a</sup>, Floury J.<sup>a</sup>, Boulier-Monthéan N.<sup>a</sup>, Prioul C.<sup>b</sup>, Dupont D.<sup>a</sup>, Nau F.<sup>a,\*</sup>

<sup>a</sup> STLO, INRA, AGROCAMPUS OUEST, 35042, Rennes, France

<sup>b</sup> Liot SAS, 86450, Pleumartin, France

\* Corresponding author: Agrocampus Ouest, UMR1253 Science et technologie du lait et de l'œuf, 65 rue de Saint-Brieuc, 35042 Rennes, France

E-mail addresses: manon.hiolle@inra.fr (Hiolle M.), valerie.lechevalier@agrocampus-ouest.fr (Lechevalier V.), juliane.floury@agrocampus-ouest.fr (Floury J.), nathalie.monthean@agrocampus-ouest.fr (Boulier-Monthean N.), claire.prioul@liot.fr (Prioul C.), didier.dupont@inra.fr (Dupont D.), francoise.nau@agrocampus-ouest.fr (Nau)

### **Abstract**

Digestion is a mechanical and chemical process that is only partly understood, and even less so for complex foods. In particular, the issue of the impact of food structure on the digestion process is still unresolved. In this study, the fate of four micronutrient-enriched foods with identical compositions but different microstructures (Custard, Pudding, Sponge cake, Biscuit) was investigated using the 3-phase *in vitro* model of human digestion developed by the INFOGEST network. Matrix disintegration and hydrolysis of macronutrients (proteins, lipids and carbohydrates) were monitored during the three phases of digestion using biochemical techniques, size-exclusion chromatography, thin-layer chromatography and gas chromatography. Micronutrient release (vitamin B9 and lutein) was monitored using reverse-phase chromatography. Food structure did not greatly influence macronutrient hydrolysis, except for lipolysis that was four-times higher for Biscuit compared to Custard. However, the bioaccessibility of both micronutrients depended on the food structure and on the micronutrient. Vitamin B9 release was faster for Biscuit and Sponge cake during the gastric phase, whereas lutein release was higher for Custard during the intestinal step. Extensive statistical analysis highlighted the impact of food structure on the digestion process, with different digestion pathways depending on the food matrix. It also made it possible to characterise the gastric step as a predominantly macronutrient solubilisation phase, and the intestinal step as a predominantly hydrolysis phase.

### **Keywords**

*In vitro* digestion; Digestion pathways; Microstructure; Nutrient release; Macronutrient hydrolysis;  
Micronutrient bioaccessibility; Food disintegration

## 1. Introduction

Food disintegration during digestion is a complex process, and although it has been thoroughly studied, it still contains some gaps of knowledge. Digestion provides nutrients to the body through the release of molecules in the gastrointestinal tract for further absorption. Whereas the nutritional quality of food was based on its nutrient profile in the past, this vision no longer applies since the matrix effect has been proven in many studies. Thus, the food matrix structure can modulate the glycaemic response (Haber, Heaton, Murphy, & Burroughs, 1977), satiety (Moorhead et al., 2006) as well as the glycaemic index (Granfeldt, Björck, & Hagander, 1991), highlighting its impact on carbohydrate digestion. With respect to proteins, the rate of amino acid absorption was shown to depend on the mode of milk gelation (rennet or acidic gels) (Barbé et al., 2014), and the structural properties of egg white gel impacted the nature and kinetics of peptide release (Nyemb-Diop et al., 2016). Similarly, technological treatments of fat such as emulsification or homogenisation can modulate chylomicron absorption and fatty acid metabolism (Gabert et al., 2011). These studies therefore suggest that, given the same composition, the organisation of nutrients within a food can directly affect the digestion process (nutrient bioaccessibility and bioavailability) with potential metabolic consequences. Consequently, understanding the fate of foods during digestion is necessary to know how they affect metabolism (Jacobs & Tapsell, 2007).

Moreover, the food matrix structure can influence micronutrient release. Lutein bioaccessibility increased by about 10% after a previous enzymatic step aimed at food structure disruption (Castenmiller, West, Linssen, van het Hof, & Voragen, 1999). A greater increase in plasma vitamin B9 (known as folate) levels was also observed after consumption of crushed spinach leaves compared to whole spinach (van het Hof, Tijburg, Pietrzik, & Weststrate, 1999). However, the majority of studies reported that food structure is not the only factor that differed between the tested foods and that is likely to influence the bioaccessibility of micronutrients. In particular, food composition was not always the same and could therefore be involved, in addition to the structure effect (de Pee & West, 1996). In the present study, we only focused on the effect of food structure on food disintegration and micronutrient release, independently of food composition.

Food structure plays a key role from the beginning of food ingestion with the chewing step (in the case of solid foods), impacting the particle size of the food bolus (Peyron, Mishellany, & Woda, 2004). Food density, texture and microstructure are also critical for particle fragmentation and hydrolysis in the gastric phase (Dekkers, Kolodziejczyk, Acquistapace, Engmann, & Wooster, 2016). This could modulate gastric emptying, leading to the difference in nutrient absorption kinetics in the intestine (Kong & Singh, 2008). Furthermore, in the stomach and small intestine compartments, the viscosity and the structure and size of solid particles may affect the enzyme diffusion into the chyme and enzyme accessibility to the substrate, impairing its activity (Blazek & Gilbert, 2010).

In order to investigate the impact of food structure on the digestion process, including an access to each digestion step (oral, gastric, intestinal), an *in vitro* static digestion model developed by the INFOGEST network was used (Minekus et al., 2014). The novelty of the present study relies on the fact that complex and realistic foods that differed only in structure, texture and water content were studied, and that the kinetics of macronutrient hydrolysis (proteins, carbohydrates and lipids) as well as micronutrient release from the matrix were recorded. For this purpose, four micronutrient-enriched food matrices were designed, with identical dry matter composition. They were enriched with a lipophilic (lutein) and a hydrophilic (vitamin B9) micronutrient in order to study the impact of their solubility on their release. Moreover, Principal Component Analysis and Multiple Factor Analysis were performed to deal with the complexity of the dataset obtained and were consequently a useful tool to study kinetics phenomena (Lechevalier et al., 2015).

## **2. Materials and methods**

### **2.1. Ingredients and reagents**

The foods were formulated with the following ingredients: wheat flour (Francine T45, Grands Moulins de Paris, Ivry Sur Seine, France); extruded dehulled pea flour (Sativa 32/100, Sotexpro, Bermericourt, France); powdered sugar (Saint-Louis Sucre, Paris, France); sunflower oil (Lesieur, Asnières-sur-Seine, France); standard pasteurised egg yolk and granulated pasteurised egg white powders (Liot, Pleumartin, France) and sterilised water. Vitamin B9 (folic acid) was supplied by Nutrilo GmbH (ref 05-050, Cuxhaven, Germany) in pure powder form. A homogeneous dispersion of lutein was prepared from capsules provided by Diet Horizon (ref. 2779, Bordeaux, France) and containing about 20 mg lutein suspended in sunflower oil; its concentration was determined by spectrophotometry at 445 nm. All reagents, unless otherwise specified, were provided by Sigma (Saint Quentin Fallavier, France) and were of analytical grade.

### **2.2. Preparation of foods**

Four foods enriched with vitamin B9 and lutein were produced according to the flowcharts and composition presented in Figure 1. The kneading, whisking and mixing steps as well as the heat treatment for Custard were carried out with a Thermomix® TM5 kitchen robot (Vorwerk, Wuppertal, Germany). Biscuit, Sponge cake and Pudding (solid foods) were cooked using a semi-professional convection oven (De Dietrich, Niederbronn-Les-Bains, France). The dry matter in the food consisted of 17% proteins, 52% carbohydrates and 30% lipids. Food lipid content was controlled by lipid weighing after Folch extraction, and protein content by the Kjeldahl method (data not shown). Custard (liquid food) was prepared as a packed powder to be rehydrated and heated at the time of use. Pudding, Sponge cake, and Biscuit were stored at -20°C until use and then defrosted at room temperature.

### **2.3. Confocal microscopy and image analysis**

For Biscuit, 300- $\mu\text{m}$ -thick cryosections mounted in OCT (Optimal Cutting Temperature) compound were transferred onto glass slides. For Sponge cake and Pudding, 300- $\mu\text{m}$ -thick microsections mounted in paraffin were cut and transferred onto glass slides. CLSM observation was performed using a ZEISS LSM 880 inverted confocal microscope (Carl Zeiss AG, Oberkochen, Germany) set at the magnification of  $\times 20$  (Plan Apochromat objective, dry, NA 0.80). The protein network and fat components were stained using a 1% (w/v) Fast Green aqueous solution and a 0.1% (w/v) Nile Red 1,2-propanediol solution, respectively (Sigma Aldrich, St. Louis, MO, USA). Both fluorescent solutions were first mixed at a ratio of 1:4. Ten  $\mu\text{L}$  of this mix were then either deposited on the surface of the slice for the solid matrices or directly added to 100  $\mu\text{L}$  of the Custard and vortexed. The samples were kept at 20°C for at least 10 min to permit the diffusion of the fluorescent dyes into the solid matrices. One drop of the labelled Custard was deposited on a glass slide. A cover slip sealed with an adhesive frame (Geneframe, ABgene House, UK) was then added on top of the four different product slices before observation using 488 and 633 nm excitation wavelengths in sequential beam fluorescent mode, for fat and protein detection, respectively, at a 1.32  $\mu\text{s}$  pixel dwell scanning rate. Red Nile and Fast Green were detected using a GaasP between 500 and 585 nm and a PMT between 635 and 735, respectively. Micrographs had a resolution of 0.15  $\mu\text{m}/\text{pixel}$  and were recorded in the samples at a constant depth of 10 to 15  $\mu\text{m}$  from the glass slide. Images shown in this paper correspond to superimpositions of images of the same area observed separately with the two markers, with proteins coded in green and fat in red. Aqueous phases and any gas bubbles in the slices may appear as black holes in the micrographs. There were at least two samples of each product, and at least 16 micrographs were recorded for each sample. The micrographs presented in Figure 3 were considered to be representative of the different product samples.

Confocal micrographs of the Red Nile-stained lipid droplets of the different matrices (channel 2) were converted to binary images using the “Otsu” thresholding algorithm of Fiji-win64 software (Image J 1.51n, National Institutes of Health, USA). The segmentation procedure was validated by visual comparison of the resulting binary image with its original image. The particle areas and perimeters were measured using the Analyze Particles measurement tool (in  $\mu\text{m}^2$ ), and the data generated were analysed according to Bornhorst, Kostlan, & Singh (2013). For each product, the cumulative lipid droplet area was calculated for each image, for each predetermined particle size. The cumulative area percentage covered by lipid droplets was then plotted against the particle area in order to determine the median particle area.

### **2.4. *In vitro* static digestion**

*In vitro* digestions were carried out according to the standardised INFOGEST protocol (Minekus et al., 2014). Triplicates were performed on three batches of each food prepared independently and randomised. The enzymatic activities of individual enzymes and pancreatin, as well as the bile salt concentration in the bovine bile extract, were determined according to Minekus et al. (2014).

Foods were either defrosted (Biscuit, Sponge cake or Pudding) or prepared (Custard) before digestion. Water content differences between the foods were offset by water addition up to the Custard water content, so that the digestion proceeded at a constant enzyme-to-dry matter ratio for all the foods. For solid foods, a preliminary step of chewing simulation was applied using a stomacher for two cycles of 30 s at 380 rpm (Mixwel +, Awel Microbiology). Custard was not subjected to mastication due to its liquid texture.

After chewing, the protocol was the same for all of the matrices. The oral bolus was prepared by mixing 7.98 g of the liquid or masticated and diluted foods with 2.58 mL of pure liquid human saliva (Lee Biosolutions 991-05-P, amylase activity of 356 U/mL), and was incubated for 2 min at 37°C in a water bath under constant stirring at 80 rpm.

The oral bolus was then mixed with 8.45 mL simulated gastric fluid (SGF), 5.3 µL of 0.3M CaCl<sub>2</sub>, 500 µL of 1M HCl (to adjust the pH to 3), and 610 µL of distilled water. After the addition of 1 mL porcine pepsin solution made up in SGF (42,264 U/mL; Sigma P6887), the solution was incubated for 2 h at 37°C under stirring at 80 rpm. The composition of all electrolyte solutions was based on the literature (Minekus et al., 2014). Intestinal digestion immediately started by adding 8.45 mL simulated intestinal fluid (SIF), 42.3 µL of 0.3M CaCl<sub>2</sub>, 50 µL of 1M NaOH (to adjust the pH to 7), 176.4 µL of distilled water and enough bile extract solution (Sigma B3883) to obtain 10 mM bile salts in the final digestion volume. After the addition of 8.45 mL pancreatin solution made up in SIF (500 U/mL of trypsin activity, Sigma P7545), the solution was incubated for 2 h at 37°C under stirring at 80 rpm.

During each digestion, samples were taken at the beginning of the oral phase (just after saliva addition; sample S0) and at times 0, 30, and 120 min during gastric and intestinal phases (samples G0, G30, G120 and I0, I30, I120, respectively). Ten µL Pepstatin A solution (0.5 mg/mL in methanol; Sigma P5318), and 50 µL Pefabloc solution (0.1M in distilled water; Sigma P76307) were added per mL of digesta in gastric and intestinal samples, respectively, to stop proteolysis; 50 µL of 4-bromophenylboronic acid (0.1M in methanol, Sigma B75956) were added per mL of digesta to inhibit lipolysis. All samples were centrifuged at 1,000 *g* at 4°C for 5 min; both supernatants were collected (oil and aqueous phases), vortexed to form an emulsion, henceforth referred to as digesta, and stored at -80°C until further analysis.

## **2.5. Physicochemical analysis**

### **2.5.1. Protein analysis and proteolysis**

### **2.5.1.1. Nitrogen and free primary amino group quantification**

The total nitrogen content of the digesta was determined using the micro-Kjeldahl method (Miller & Houghton, 1945). The rate of proteolysis during digestion was assessed by measuring the free primary amino groups in the soluble fraction of digesta using the o-phthaldialdehyde (OPA) spectrophotometric assay in microplates (Darrouzet-Nardi, Ladd, & Weintraub, 2013).

### **2.5.1.2. Molecular weight distribution of the soluble fraction of digesta**

The molecular weight distribution of the soluble peptides released during digestion was determined by Size Exclusion Chromatography (SEC). Digesta were diluted in phosphate buffer (50 mM, pH 7, 0.2M NaCl) and filtered through 0.2- $\mu$ m pore-size filters before injection onto a BioSep-SEC-S2000 Phenomenex column connected to a Waters e2695 separation module equipped with a Waters e2489 UV/Visible detector (Waters Corporation, Milford, MA, USA). Elution was performed under an isocratic 0.8 ml/min flow of phosphate buffer (50 mM, pH 7, 0.2M NaCl) at 37°C, with detection at 214 nm. Preliminary calibration of the chromatographic system with seven molecular weight markers (bovine thyroglobulin, 670 kDa; IgG from human gamma globulin, 150 kDa; ovalbumin, 44 kDa; myoglobin, 17 kDa; cytochrome from horse heart, 12.38 kDa; aprotinin, 6.51 kDa; angiotensin II human, 1.05 kDa) made it possible to quantify the proportion of proteins and peptides (corresponding to the Area Under the Curve (AUC)) in seven molecular weight ranges: >100 kDa, 100-50 kDa, 50-25 kDa, 25-10 kDa, 10 -5 kDa, 5-1 kDa and < 1 kDa, respectively referred to as classes 1 to 7.

### **2.5.2. Amylolysis characterisation**

Amylolysis was determined as the quantity of oligosaccharides (polymerisation degree of 10 or less) solubilised in the digesta and estimated as previously described by Freitas & Le Feunteun (2019).

### **2.5.3. Lipid analysis and lipolysis**

#### **2.5.3.1. Free fatty acid quantification**

Lipids from digesta were extracted according to the Folch method, acidified with 160  $\mu$ L of 0.1M HCl (Folch, Lees, & Sloane Stanley, 1957). Free fatty acids (FFA) were isolated using a solid-phase extraction column (Macherey-Nagel 730033G) and then methylated with BF<sub>3</sub> (14% in methanol) at 70°C for 15 min. Fatty acid methyl esters (FAME) were extracted with pentane and analysed on an Agilent gas chromatograph (7890A) equipped with a BPX70 capillary column and coupled to a flame ionisation detector (Agilent Technologies, Les Ulis, France). Components were identified according to the retention time of authentic FAME standards. FFA concentrations were calculated using an internal standard (80  $\mu$ g of C17). The lipolysis degree was expressed as the percentage of FFA released at a



given time vs. the total quantity of FA digested. For this purpose, total lipids from foods were extracted and analysed as described above.

#### **2.5.3.2. Quantification of lipid classes**

The lipid classes (extracted from digesta) were separated on silica thin layer chromatography (TLC) plates using hexane:diethyl ether:acetic acid (70:30:1, v:v) as the eluent. The lipid bands were visualised by spraying the plates with a 10% (w/v) cupric sulphate solution in 8% (w/v) orthophosphoric acid and heating for 10 min at 150°C. After scanning using a Labscan (GEHealthcare, ImageScanner III), the band density was estimated using Image J software. Six classes were separated: Triglycerides (TAG), Free Fatty Acids (FFA), Cholesterol (CHOL), Diglycerides (DAG), Monoglycerides (MAG) and Phospholipids (PL). Lipolysis could therefore be estimated prior to the ultimate stage of FFA.

#### **2.5.3.3. Total lipid quantification**

The total acyl chains present in residual glycerides (henceforth referred to as total lipids) were quantified from digesta using a Biomérieux kit (Craponne, France).

#### **2.5.4. Vitamin B9 quantification**

Vitamin B9 was extracted from digesta with a single-use folic acid immunoaffinity column (R-biopharm P81B). Subsequently, the column was washed with 10 ml distilled water before the vitamin was eluted, first with 1 mL of an acetonitrile:trifluoroacetic acid (30%:0.2% v:v) solution, and then with 1 mL distilled water. The two eluates were pooled together in an amber vial and analysed for vitamin B9 quantification by RP-HPLC using a ThermoScientific system (Dionex Ultimate 3000) equipped with a Symmetry C18 column (150 × 2.1 mm; particle size: 5 µm; Waters) and a UV spectrophotometer (Dionex Ultimate 3000). A 29-min gradient was applied with solvent A (0.1% trifluoroacetic acid) and solvent B (acetonitrile + 0.1% trifluoroacetic acid). Gradient conditions were initially 12% B for 2 min, increased linearly to 20% B over 2 min, maintained for 5 min, then increased linearly to 75% B over 1 min, maintained for 4 min and returned to 12% B in 15 min. The flow rate was 0.2 mL/min, the column temperature 30°C, and the injection volume 100 µL. Absorbance was measured at 280 nm and vitamin B9 was quantified using an external calibration curve.

#### **2.5.5. Lutein quantification**

Lutein was extracted from digesta according to Kopec, Gleize, Borel, Desmarchelier, & Caris-Veyrat (2017). Extracts were then dissolved in 50 µL dichloromethane and 50 µL methanol for lutein analysis by RP-HPLC using a Thermo Fisher system (Finnigan Surveyor) equipped with a C18 column (250 × 4.6

mm; particle size: 5 µm; Grace/Vydac 201TP) and a photodiode array detector (PDA Plus Detector). The composition of solvents was (A) methanol:0.05M ammonium acetate (80:20, v:v), (B) acetonitrile:distilled water (90:10, v:v), and (C) pure ethyl acetate. Gradient conditions were initially 100% A, increased linearly to 100% B in 2 min, then to 100% C in 22 min, returned to 100% B in 2 min, then to 100% A in 4 min. The flow rate was 1 mL/min and the column temperature was 25°C. Absorbance was measured at 445 nm. Lutein and echinenone were quantified using external calibration curves generated from authentic standards (Sigma 07168 and 73341, respectively). Due to the tendency of lutein to degrade under experimental digestion conditions (acidic pH and heat), quantification was performed on both the supernatant and total sample at each sampling time (Kopeck et al., 2017). Lutein bioaccessibility was expressed as the percentage of lutein released in the supernatant at a given time vs. the total quantity of lutein present in the whole sample at the same given time.

## **2.6. Statistical analysis**

From the analyses described above, a dataset of 21 columns (21 variables described in Table 1) and 84 rows (84 samples) was obtained.

### **2.6.1. ANOVA**

ANOVA tests were used to determine the impact of matrix, time and their interaction on each variable. The linear model procedure of R was applied to determine  $R^2$  and the p-value of the following modelling:  $Y = \text{Matrix} + \text{Time} + \text{Matrix} * \text{Time}$ . Differences were considered significant at a minimum level of 95%. Residual normality and variance homogeneity were tested for each variable using a Shapiro-Wilk test and a Brown-Forsythe test (R Development Core team, 2007), respectively.

### **2.6.2. Principal component analysis**

A Principal Component Analysis (PCA) was performed on the whole dataset to highlight the correlations between the variables and to characterise the evolution of the four foods during digestion in view of these variables. PCA and all the following statistical analyses were performed using the FactoMineR package of R software 3.5.2 (Lê, Josse, & Husson, 2008; R Development Core team, 2007). "Digestion time" was added as a supplementary variable. The variables were automatically standardised (mean centred and scaled) by the software to give them all the same importance.

### **2.6.3. Hierarchical clustering analysis**

Hierarchical clustering analysis (HCA) is a statistical method designed to highlight the similarities between individuals. It creates clusters of alike individuals by maximising the inter-cluster differences

and minimising the intra-cluster differences. HCA was performed on the results of PCA using Ward's method for hierarchical clustering with the Euclidean distance as a similarity measure. Only the five first principal components were taken into account to suppress the noise contained in the last principal components.

#### **2.6.4. Multiple factor analysis**

To overcome the digestion time effect, a Multiple Factor Analysis (MFA) was carried out. Briefly, variables were separated into subgroups depending on digestion time and a PCA was performed on each of these subgroups (see Supplementary Materials 2). The results of all these PCA were then represented in a common space that makes it possible to compare them (Lechevalier et al., 2015).

### **3. Results and discussion**

#### **3.1. Food processing generated strong differences in macro- and microstructures of the four foods**

The differences in processing conditions and water content (Figure 1) resulted in four foods that differed by their macroscopic aspect. The Biscuit was a very dry and brittle product. The Sponge Cake was an airy, soft, and dry gel. The Pudding consisted of a humid and compact gel. Finally, the Custard was a thick liquid (Figure 2).

Confocal microscopy images of the four foods showed a uniform green background with Biscuit, Sponge cake and Pudding, suggesting a continuous protein phase in these three foods. It was expected that protein and starch should be the main components of the molecular network of these solid foods. However, the protein phase seemed to be disrupted in several locations in the Sponge cake and Pudding structures, probably due to non-homogenous mixing. In Custard, small particles with a diameter of about 50  $\mu\text{m}$  could be seen, suggesting protein aggregation.

With regard to the lipid phase, Custard and Biscuit contain bigger lipid droplets than Sponge cake and Pudding, in which lipids are more diffuse. However, lipids are very globular in Custard, whereas puddles of fat are present in Biscuit. The bigger apparent size of lipid droplets for Biscuit is in line with the distribution of the lipid droplet area (Figure 3E). With regard to Custard, despite the existence of some large lipid droplets, most of the lipid droplets are much smaller (around 10  $\mu\text{m}$  in diameter), thus explaining that Custard had the lowest median area of lipid droplets amongst the four foods. Sponge cake and Pudding are intermediate with regard to the median area of lipid droplets. The  $b$  constant, indicative of distribution spread, follows the opposite trend of the medians: it is greater in Custard (1.08), followed by Pudding (0.46), Sponge cake (0.38) and then Biscuit (0.25). Custard then has the narrowest size distribution. Therefore, despite the few large lipid droplets observed on confocal

images, Custard is in fact mainly composed of very small droplets. Biscuit has the widest size distribution and therefore presents both large and small droplets. As a conclusion, the four designed foods strongly differ in both their microstructure and macrostructure.

### **3.2. Food disintegration assessed through macronutrient release and hydrolysis during *in vitro* digestion**

#### **3.2.1. Peptide solubilisation and proteolysis mainly occur during the intestinal phase**

The kinetics of proteolysis were assessed from the release of soluble proteins and peptides (estimated by total soluble nitrogen) and from free amino groups in the supernatant throughout the three phases of *in vitro* digestion. Kinetics of peptide solubilisation are equivalent for the four foods (Figure 4A). Most of the peptide solubilisation occurs within the first few minutes of the intestinal phase due to the combined effect of bile salts and pancreatin addition (only 28% at the end of the gastric phase). This is typically observed with protein-rich matrices submitted to the INFOGEST protocol (Lorieau et al., 2018; Minekus et al., 2014). Peptide solubilisation then further increases before a plateau is reached after 160 min digestion.

At the end of the gastric phase, the quantity of free amino groups released constitutes only some 14% of the total free amino groups released at the end of the whole digestion (Figure 4B), whereas 28% of the total nitrogen is released at this step (Figure 4A). This suggests that food disintegration (protein solubilisation) more than proteolysis of soluble material (free amino group release) occurs during gastric digestion. On the contrary, free amino groups further increase beyond 160 min digestion, whereas the quantity of soluble peptides remains constant, suggesting that proteolysis of soluble peptides occurs until the end of the intestinal phase.

Protein digestibility may depend on their degree of denaturation (Jin et al., 2016), food processing can modify the digestion and absorption kinetics of nutrients (Morell, Fiszman, Llorca, & Hernando, 2017), and food microstructure may affect the rate or extent of protein digestion (Barbé et al., 2013; Nyemb et al., 2016; Rinaldi, Gauthier, Britten, & Turgeon, 2014). However, in the present study, no significant difference between the four foods was observed, neither on proteolysis nor on peptide release from the food matrix. Thus, these results are in agreement with Lorieau et al. (2018) who reported the same rate of proteolysis for whey protein heat-induced gels, differently structured but with identical composition, when submitted to simulated intestinal digestion. Luo, Boom, & Janssen (2015) observed that the gel structure may alter the reaction rate and mechanisms of pepsinolysis and assumed that the difference in pepsin activity stemmed from the steric hindrance of gel structure to the diffusion of pepsin. Nyemb et al. (2016) suggested a similar hypothesis to explain the discrepancy between four different egg white gels during *in vitro* digestion. Therefore, despite the different microstructures of

the four foods studied here, the diffusion of digestive proteases might not be significantly impacted, leading to comparable kinetics of proteolysis.

### **3.2.2. Amylolysis starts during the oral phase but essentially occurs during the intestinal phase**

Figure 5 shows the kinetics of oligosaccharide release during *in vitro* digestion, which are similar for the four foods. As expected, oligosaccharide release first occurs during the oral phase despite the fact that it is a very short step (2 min) (Figure 5, insert), due to the action of  $\alpha$ -amylase from human saliva. Amylase activity stopped when entering the gastric phase due to the drop in pH since this enzyme is no longer active at a pH lower than 3.8 (Freitas, Le Feunteun, Panouillé, & Souchon, 2018; Nielsen, Borchert, & Vriend, 2001). Immediately after pancreatin addition, oligosaccharide release suddenly increases due to the action of pancreatic  $\alpha$ -amylase, as previously observed by Freitas & Le Feunteun (2019). Soluble oligosaccharides further increase until the end of the intestinal phase, despite a slowdown after 150 min digestion.

Previous studies indicate that starch digestion should not be affected by cooking conditions (equivalent to the degree of starch gelatinisation), but rather by the natural characteristics of starch microstructure like cell shape, size or wall composition (Singh, Kaur, & Singh, 2013; Tamura, Singh, Kaur, & Ogawa, 2016). However, the increase in digesta viscosity has been shown to impact starch digestion by hampering interactions between substrates (starch and oligosaccharide) and digestive enzymes (salivary and pancreatic amylases) (Singh, Dartois, & Kaur, 2010; Singh et al., 2013). Proteins in the food matrix tend to interact with starch as well, lowering its digestibility (Ezeogu, Duodu, Emmambux, & Taylor, 2008). Finally, FFA released during digestion can interact with starch and form a complex that is resistant to amylases (Seligman, Copeland, Appels, & Morell, 1998). The sum of all these effects, potentially conflicting, could explain why similar kinetics of amylolysis were observed here, regardless of the food.

### **3.2.3. Lipid release and lipolysis mainly occur during the intestinal phase**

The fate of lipids during *in vitro* digestion was approached by means of two variables: the quantity of lipids released in the soluble fraction of digesta, indicative of food disintegration, and the ratio of FFA to the total FA, indicative of lipolysis. The kinetics of both variables are presented in Figure 6.

At 32 min and 153 min of digestion, which corresponded to 30 min of gastric and intestinal phases, respectively, lipid solubilisation significantly differed between the four foods (Figure 6A). Whereas lipid solubilisation tends to be the highest for Biscuit and the lowest for Sponge cake and Pudding during the gastric phase, the opposite behaviour is observed during the intestinal phase. Moreover, just as for peptide solubilisation (Figure 4A), lipid solubilisation strongly increases at the very beginning of the intestinal phase, confirming severe food disintegration early in this phase.

Lipolysis curves are completely different from lipid solubilisation curves since no lipolysis occurs during the gastric phase (Figure 6B). Moreover, the lipolysis rate significantly differs between the four foods during the intestinal phase. Custard presents a much lower lipolysis throughout this phase. Although Sponge cake, Pudding, and Biscuit present similar lipolysis during the first 30 min, differences progressively increase. At the end of intestinal digestion, Biscuit exhibits 100% lipolysis, vs 65% for Sponge cake, 54% for Pudding and 28% for Custard.

Thus, the present results are not in agreement with those reported by Mat, Le Feunteun, Michon, & Souchon (2016) who observed different kinetics of lipolysis in liquid and solid emulsions, with a faster rate of lipolysis during the first minutes of digestion for the liquid one compared to the solid one. These authors assumed that lipase diffusion to the substrate is slowed down in solid emulsions compared to liquid emulsions, leading to slower lipolysis kinetics. To explain such a difference in digestion kinetics, Luo et al. (2015) introduced the concept of a “zipper” mechanism for liquid matrices (fast initial hydrolysis followed by a steadier stage), in opposition to a “one-by-one” mechanism for solid matrices (slow initial rate followed by a more-sustained trend during intestinal digestion). According to this concept, the kinetics observed in the present study tend to follow the “one-by-one” mechanism, even for the liquid matrix. This could result from some protein aggregation in Custard during the gastric phase because of the acidic conditions, the matrix then acting locally as a solid gel (Alting et al., 2004). Nevertheless, the high rate of lipolysis observed for the Biscuit is still surprising, especially since the lipid droplet size is the highest in this matrix (Figure 3), meaning a lower surface/volume ratio in comparison with the other foods, which is unfavourable for lipolysis (Golding et al., 2011). In fact, recent studies demonstrated that the homogenisation of milk resulted in a higher rate of lipolysis (Islam et al., 2017). However, the slower lipolysis kinetics of the three other foods could be due to some lipid coalescence or flocculation during the digestion process, thus decreasing the interface area effectively available for the lipase action, despite initial smaller fat globules (Day et al., 2014; Giang et al., 2015). This hypothesis is compatible with the puddles of fat observed at the surface of digesta during the experiments (data not shown).

In a similar study that implemented a semi-dynamic system, similar observations were made regarding the rate of lipolysis in liquid vs. solid food matrices. In the liquid sample, a phase separation occurred during the gastric phase due to creaming, whereas it was very limited in the semi-solid matrix, resulting in a lower lipolysis at the end of digestion of the liquid emulsion (Mulet-Cabero, Rigby, Brodkorb, & Mackie, 2017).

### **3.3. Micronutrient bioaccessibility depends on food characteristics and on the considered micronutrient**

The kinetics of vitamin B9 release during digestion are slightly different for the four foods (Figure 7A). During the oral phase, a sharp increase in soluble vitamin B9 is observed, but without any difference between the foods. Two types of behaviour then occur in the gastric phase: vitamin B9 release is higher for Biscuit and Sponge cake during the first 30 min before reaching a plateau, whereas a continuous increase occurs for 120 min for Custard and Pudding. At the end, no difference of total vitamin B9 release exists between the four foods. When entering the intestinal phase, a brutal and substantial decrease of soluble vitamin B9 is noted for Biscuit, Pudding, and Custard, as well as, to a lesser extent, for Sponge cake. The insolubilisation of vitamin B9 is probably due to the rise in pH from 3 to 7 since vitamin B9 is very poorly soluble at neutral pH (Wu, Li, Hou, & Qian, 2010).

With regard to lutein, similar release kinetics in the soluble fraction of the digesta are observed for the three solid foods, whereas the liquid food behaves differently during the oral and intestinal phases (Figure 7B). The difference already exists in the products before digestion: around 20% of lutein is in the soluble fraction for Custard, whereas lutein is almost completely entrapped in the solid fraction for Biscuit, Sponge cake and Pudding. The release of lutein during the oral phase is however limited in all of the cases, resulting in a higher percentage of soluble lutein in Custard compared to the solid foods. When entering the gastric phase, the percentage of soluble lutein decreases during the first 30 min for Custard, reaching values similar to those of the three solid foods; at the end of the gastric phase, the bioaccessibility of lutein reaches about 25% for the four foods. During the intestinal phase, the rate of lutein bioaccessibility continues to increase up to 55% for Custard, while remaining constant at 25% for the three solid foods.

The food matrix is known to play a role in vitamin B9 absorption. Castenmiller et al. (2000) reported that the disruption of the spinach matrix by mincing improves vitamin B9 bioavailability. Similar results were found for microwaved chopped compared with microwaved whole spinach (van het Hof et al., 1999). The network formed by dietary fibers might be responsible for these differences (Ristow, Gregory, & Damron, 1982). However, in the present study, there is no fiber network likely to hinder vitamin B9 release, which could explain that no difference was observed between the four foods regarding vitamin B9 bioaccessibility, despite apparently different behaviours in the gastric phase.

Gleize et al. (2013) observed that lutein bioaccessibility was greater when provided by a diet mainly containing short FA rather than mono- or polyunsaturated FA because the first one produced smaller mixed micelles. Although the four foods studied here initially contained the same FA composition, the differences in lipolysis observed (the highest for Biscuit, the lowest for Custard; see Figure 5B) may lead to some differences in terms of FA released, with potential consequences on the size of the mixed micelles produced and, consequently, on lutein bioaccessibility. Another hypothesis is that the lipid droplet size and, thus, the surface area for exchange between the oil and aqueous phases, could affect the transfer efficiency of lutein from the food matrix to the soluble phase (Reboul et al., 2006).

Although Custard presents the smallest lipid droplets amongst the four foods (Figure 3E), the evolution of the lipid size distribution during *in vitro* digestion remains unknown, making the validation of this hypothesis impossible. A third hypothesis is a potential effect of lipolysis on the lutein transfer into the soluble phase. Indeed, carotenoids like lutein require the presence of lipids in the soluble phase in order to be released from the food matrix (Tyssandier et al., 2003). This hypothesis seems to be reasonable here since a significant matrix effect was observed on lipolysis and a strong relationship exists between the total lipid content in the soluble phase during digestion and lutein release, which could primarily result from its lipophilic nature (correlation coefficient = 0.60; p-value < 0.0001).

#### **3.4. The food matrix strongly influences the markers of digestion**

The effect of the food matrix and digestion time on the different characteristics of the digesta was tested by ANOVA. Based on the linear model analysis (Table 2), all the variables tested significantly changed with the food matrix except for vitamin B9 release, and with digestion time except for cholesterol release and a specific class of peptide molecular size. Therefore, even if the food matrix may be a determining variable at a certain given digestion time for almost all of the characteristics of the *in vitro* digesta, differences in the digestion kinetics may also exist, in addition to the expected effect of digestion time. It is then reasonable to assume that the food matrix has an impact on the digestion process.

#### **3.5. The gastric phase is primarily a macronutrient solubilisation step, whereas the intestinal phase is a hydrolysis step**

In order to highlight correlations between the food matrix, digestion time, and all the characteristics measured on the digesta, a principal component analysis (PCA) was carried out (Figure 8A). The first two principal components (PCs) account for a cumulative variability of 72%. A significant portion of the information provided by the dataset could thus be plotted in 2D defined by PC1 and PC2.

PC1 (60.74% of the variability) is positively correlated with markers of food disintegration (total lipids and peptides released in the soluble fraction), but also with markers of lutein release and of macronutrient hydrolysis: lipolysis (FFA, MAG, DAG measured by TLC and lipolysis degree measured by GC), amylolysis (oligosaccharides released), proteolysis (free amino groups and all classes of peptides < 25 kDa); PC1 is negatively correlated with triglycerides. PC2 (11.78% of the variability) is positively correlated with TG, cholesterol, proteins >100 kDa and vitamin B9 release, all of which are markers of food disintegration. According to the matrix of Pearson's correlation (Supplementary Material 1), markers of food disintegration and those of macronutrient hydrolysis are strongly correlated. Furthermore, these two phenomena are correlated with the time of digestion, indicating that they take place at the same time.



The graph of the individuals on PC1 and PC2 does not make it possible to show any impact of the food matrix on the digestion process, as confirmed by the barycentre's of the four matrices, which are very close to each other and to the centre of the graph (Figure 8B). However, when analysed from the point of view of digestion time, PC1 and PC2 make it possible to split the samples according to the phases of *in vitro* digestion (Figure 8C). Digesta collected at the very beginning of the salivary phase (S0) have the lowest coordinates on PC1 and PC2, indicating the lowest food disintegration, macronutrient hydrolysis and micronutrient release. During the gastric phase (from G0 to G120), the sample coordinates increase on PC2, meaning that the *in vitro* gastric phase mainly consists of solubilising the macronutrients. In this way, TG and high molecular weight peptides become more and more abundant in the soluble fraction of the digesta, and are then accessible for further hydrolysis by digestive enzymes. During the intestinal phase (from I0 to I120), sample coordinates then decrease on PC2 and increase on PC1, indicating the progressive disappearance of TG and high molecular weight peptides in the soluble fraction in favour of markers of macronutrient hydrolysis, as demonstrated by the increase in oligosaccharides, FFA and peptides of low molecular weight. Vitamin B9 positively correlates with PC1, i.e., its release mainly occurs during the gastric phase, whereas lutein positively correlates with PC2, i.e., its release mainly occurs during the intestinal phase, consistent with the results reported above (Section 3.3).

To carry out the PCA, a hierarchical clustering analysis (HCA) was done in order to visualise and highlight the similarities between individuals. It defined four clusters (Figure 9). The first cluster comprises 83% of the digesta collected at the beginning of the salivary phase and 100% of the digesta from the beginning of the gastric phase. Most of the remaining samples collected during the gastric phase (58% of G30 and 100% of G120 samples) constitute the second cluster. The third cluster contains almost all the digesta collected at the beginning of the intestinal phase (92% of ten samples). Finally, the fourth cluster encompasses the digesta from the rest of the intestinal phase (100% of I30 and I120). Thus, HCA analysis makes it possible to determine the key events of *in vitro* digestion: the addition of pepsin (switch from cluster 1 to cluster 2), the increase in pH from 3 to 7 (from cluster 2 to 3), and the addition of pancreatin (from cluster 3 to 4). Some events seemed to have no or little impact on the digestion process, like the addition of amylase at the beginning of the oral phase or the drop in pH from 6.5 to 3 when entering the gastric phase.

### **3.6. The impact of food on digestion pathways investigated by MFA**

A multiple factor analysis (MFA) was carried out on the dataset in order to supplement the representation of the barycentre of the food matrices with seven partial points for each food matrix (Figure 10). Each partial point corresponds to the considered food described by all of the variables at a given digestion time (S0, G0, G30, G120, I0, I30 or I120).

The first two PCs explain a cumulative variability of 77%. PC1 (48.97%) is positively correlated with markers of matrix disintegration (total soluble peptides and lipids), proteolysis (peptides of molecular weight < 25 kDa, and free amino groups released), the degree of lipolysis and lutein release. It is negatively correlated with amylolysis (oligosaccharides) and PL. PC2 (27.98%) is negatively correlated with vitamin B9 release and lipolysis (FFA, DAG, MAG) and positively correlated with peptides of high molecular weight (> 25 kDa). The significant correlation coefficients of variables at a given digestion time with the two first PCs are given in Supplementary Material 3.

The barycentre of the Biscuit cluster is located on the right side of PC1, whereas the three other foods are on the left side. This could result from lipolysis since when considering the variables correlated with PC1, lipolysis is the main phenomenon discriminating the four foods (Figure 6). Regarding Custard, Pudding and Sponge cake, these three food matrices are separated along PC2. Considering the variables correlated with PC2, it is not possible to provide an explanation for this observation. Nonetheless, the positions of the four matrix barycentres, representative of the global matrix effect, are relatively distant between each other (Figure 10), demonstrating that the food matrix strongly impacts the digestion process.

The digestion patterns, as described by the pathway of partial points throughout digestion, show that the four foods have different behaviours during *in vitro* digestion. Taking the example of Custard, at the beginning of digestion (S0), the partial point coordinates are high on PC2, meaning a high macronutrient content in the supernatant, consistent with the liquid texture and high solubility in this food. The macronutrients are then already accessible for digestive enzymes from the start of digestion. During the gastric phase, the partial point coordinates decrease on PC2, indicating some insolubilisation, probably due to the decrease in pH that could induce protein precipitation; some aggregation was actually observed. Between the end of the gastric phase and the beginning of the intestinal phase, the partial point coordinates increase on PC2, suggesting a new step of protein solubilisation. Then, during the intestinal phase, partial point coordinates increase on PC1, indicative of significant lipolysis and proteolysis during this step of digestion, consistent with the results reported above (Figures 4 and 6).

Pudding presents a different pathway, with partial point coordinates on PC2 that are lower at the beginning of the oral phase and increase during the gastric phase, indicating that the acidic pH and/or pepsin activity may lead to macronutrient solubilisation. Partial point coordinates for Custard and Pudding are very close at this step of digestion, meaning that the gastric stage tends to standardise the samples. However, the intestinal phase increases the dispersion of partial points for Pudding and Custard. Hence, although Pudding and Custard seem to be the closest matrices in terms of texture, their fate throughout digestion is very different. Digestion pathways are also very different for Sponge

cake and Biscuit, meaning that the influence of food structure on food disintegration and nutrient release results from a global and complex process.

#### **4. Conclusions**

This study highlights the influence of the food matrix structure (from liquid to hard solid) on *in vitro* digestion using a simulated gastro-intestinal model. Through different processing conditions, four foods (Custard, Pudding, Sponge cake, Biscuit) were prepared with identical compositions but with strong differences in terms of macro- and microstructure, especially regarding the size distribution of lipid droplets. The release and hydrolysis of all macronutrients (starch, proteins, lipids) mainly occurred during the intestinal step of the *in vitro* digestion. Moreover, the different matrix structures did not seem to have a great influence on macronutrient hydrolysis kinetics, except for the lipolysis rates, which were almost four times higher for the harder matrix (Biscuit) in comparison with the liquid one (Custard). However, the matrix structure influenced the bioaccessibility of both micronutrients, but in a different way. The kinetics of vitamin B9 release were impacted during the gastric phase only, with a faster release for Biscuit and Sponge cake, whereas the kinetics of lutein release were impacted during the intestinal phase only, resulting in a higher bioaccessibility for Custard.

In the end, ANOVA highlighted the overall impact of food structure on digestion kinetics, therefore suggesting an impact on the digestion process itself. This result was supported by Multiple Factor Analysis that revealed very different digestion pathways from one food matrix to another. By using a Principal Component Analysis, the digestion process could also be broken down into the gastric step during which the major phenomenon was macronutrient solubilisation, and the intestinal step during which mainly hydrolysis occurred.

However, the static model of digestion used here does not take the dynamics of gastric emptying, acid and enzyme secretions into account. These important physiological parameters will be studied in future *in vitro* digestion studies using a dynamic model.

#### **Acknowledgements**

The authors thank J.-J. Dubois and S. Wiart-Letort for conducting part of the experiments, Liot (Pleumartin, France) and Sotexpro (Bermericourt, France) for providing raw ingredients (egg powders and pea flour, respectively), and Nutrinov (Noyal-sur-Vilaine, France) for the loan of analytical equipment. They also wish to thank Gail Wagman for her help in correcting the English.

This work was supported by the Conseil Régional de Bretagne, the National Institute of Agricultural Research (INRA) and Carnot Qualiment.

## References

- Alting, A. C., Weijers, M., de Hoog, E. H. A., van de Pijpekamp, A. M., Cohen Stuart, M. A., Hamer, R. J., de Kruif, C. G., Visschers, R. W. (2004). Acid-Induced Cold Gelation of Globular Proteins: Effects of Protein Aggregate Characteristics and Disulfide Bonding on Rheological Properties. *Journal of Agricultural and Food Chemistry*, *52*(3), 623–631. <https://doi.org/10.1021/jf034753r>
- Barbé, F., Ménard, O., Gouar, Y. L., Buffière, C., Famelart, M.-H., Laroche, B., Le Feunteun, S., Remond, D., Dupont, D. (2014). Acid and rennet gels exhibit strong differences in the kinetics of milk protein digestion and amino acid bioavailability. *Food Chemistry*, *143*, 1–8. <https://doi.org/10.1016/j.foodchem.2013.07.100>
- Barbé, F., Ménard, O., Le Gouar, Y., Buffière, C., Famelart, M.-H., Laroche, B., Le Feunteun, S., Dupont, D., Rémond, D. (2013). The heat treatment and the gelation are strong determinants of the kinetics of milk proteins digestion and of the peripheral availability of amino acids. *Food Chemistry*, *136*(3–4), 1203–1212. <https://doi.org/10.1016/j.foodchem.2012.09.022>
- Blazek, J., & Gilbert, E. P. (2010). Effect of Enzymatic Hydrolysis on Native Starch Granule Structure. *Biomacromolecules*, *11*(12), 3275–3289. <https://doi.org/10.1021/bm101124t>
- Bornhorst, G. M., Kostlan, K., & Singh, R. P. (2013). Particle Size Distribution of Brown and White Rice during Gastric Digestion Measured by Image Analysis. *Journal of Food Science*, *78*(9), E1383–E1391. <https://doi.org/10.1111/1750-3841.12228>
- Castenmiller, J. J., van de Poll, C. J., West, C. E., Brouwer, I. A., Thomas, C. M., & van Dusseldorp, M. (2000). Bioavailability of folate from processed spinach in humans. Effect of food matrix and interaction with carotenoids. *Annals of Nutrition & Metabolism*, *44*(4), 163–169. <https://doi.org/12840>
- Castenmiller, J. J., West, C. E., Linssen, J. P., van het Hof, K. H., & Voragen, A. G. (1999). The food matrix of spinach is a limiting factor in determining the bioavailability of beta-carotene and to a lesser extent of lutein in humans. *The Journal of Nutrition*, *129*(2), 349–355.
- Darrouzet-Nardi, A., Ladd, M. P., & Weintraub, M. N. (2013). Fluorescent microplate analysis of amino acids and other primary amines in soils. *Soil Biology and Biochemistry*, *57*, 78–82. <https://doi.org/10.1016/j.soilbio.2012.07.017>
- Day, L., Golding, M., Xu, M., Keogh, J., Clifton, P., & Wooster, T. J. (2014). Tailoring the digestion of structured emulsions using mixed monoglyceride–caseinate interfaces. *Food Hydrocolloids*, *36*, 151–161. <https://doi.org/10.1016/j.foodhyd.2013.09.019>
- de Pee, S., & West, C. E. (1996). Dietary carotenoids and their role in combating vitamin A deficiency: a review of the literature. *European Journal of Clinical Nutrition*, *50 Suppl 3*, S38-53.

- Dekkers, B. L., Kolodziejczyk, E., Acquistapace, S., Engmann, J., & Wooster, T. J. (2016). Impact of gastric pH profiles on the proteolytic digestion of mixed  $\beta$ lg-Xanthan biopolymer gels. *Food Funct.*, 7(1), 58–68. <https://doi.org/10.1039/C5FO01085C>
- Ezeogu, L. I., Duodu, K. G., Emmambux, M. N., & Taylor, J. R. N. (2008). Influence of Cooking Conditions on the Protein Matrix of Sorghum and Maize Endosperm Flours. *Cereal Chemistry Journal*, 85(3), 397–402. <https://doi.org/10.1094/CCHEM-85-3-0397>
- Folch, J., Lees, M., & Sloane Stanley, G. H. (1957). A simple method for the isolation and purification of total lipides from animal tissues. *The Journal of Biological Chemistry*, 226(1), 497–509.
- Freitas, D., & Le Feunteun, S. (2019). Oro-gastro-intestinal digestion of starch in white bread, wheat-based and gluten-free pasta: Unveiling the contribution of human salivary  $\alpha$ -amylase. *Food Chemistry*, 274, 566–573. <https://doi.org/10.1016/j.foodchem.2018.09.025>
- Freitas, D., Le Feunteun, S., Panouillé, M., & Souchon, I. (2018). The important role of salivary  $\alpha$ -amylase in the gastric digestion of wheat bread starch. *Food & Function*, 9(1), 200–208. <https://doi.org/10.1039/C7FO01484H>
- Gabert, L., Vors, C., Louche-Pélessier, C., Sauvinet, V., Lambert-Porcheron, S., Draï, J., Laville, M., Désage, M., Michalski, M.-C. (2011).  $^{13}\text{C}$  tracer recovery in human stools after digestion of a fat-rich meal labelled with [1,1,1- $^{13}\text{C}$ ]tripalmitin and [1,1,1- $^{13}\text{C}$ ]triolein. *Rapid Communications in Mass Spectrometry: RCM*, 25(19), 2697–2703. <https://doi.org/10.1002/rcm.5067>
- Giang, T. M., Le Feunteun, S., Gaucel, S., Brestaz, P., Anton, M., Meynier, A., & Trelea, I. C. (2015). Dynamic modeling highlights the major impact of droplet coalescence on the in vitro digestion kinetics of a whey protein stabilized submicron emulsion. *Food Hydrocolloids*, 43, 66–72. <https://doi.org/10.1016/j.foodhyd.2014.04.037>
- Gleize, B., Tourniaire, F., Depeyaz, L., Bott, R., Nowicki, M., Albino, L., Lairon, D., Kesse-Guyot, E., Galan, P., Hercberg, S., Borel, P. (2013). Effect of type of TAG fatty acids on lutein and zeaxanthin bioavailability. *British Journal of Nutrition*, 110(1), 1–10. <https://doi.org/10.1017/S0007114512004813>
- Golding, M., Wooster, T. J., Day, L., Xu, M., Lundin, L., Keogh, J., & Clifton, P. (2011). Impact of gastric structuring on the lipolysis of emulsified lipids. *Soft Matter*, 7(7), 3513. <https://doi.org/10.1039/c0sm01227k>
- Granfeldt, Y., Björck, I., & Hagander, B. (1991). On the importance of processing conditions, product thickness and egg addition for the glycaemic and hormonal responses to pasta: a comparison with bread made from “pasta ingredients.” *European Journal of Clinical Nutrition*, 45(10), 489–499.
- Haber, G. B., Heaton, K. W., Murphy, D., & Burroughs, L. F. (1977). Depletion and disruption of dietary fiber. *The Lancet*, 310(8040), 679–682. [https://doi.org/10.1016/S0140-6736\(77\)90494-9](https://doi.org/10.1016/S0140-6736(77)90494-9)

- Islam, M. A., Devle, H., Comi, I., Ulleberg, E. K., Rukke, E.-O., Vegarud, G. E., & Ekeberg, D. (2017). Ex vivo digestion of raw, pasteurised and homogenised milk – Effects on lipolysis and proteolysis. *International Dairy Journal*, *65*, 14–19. <https://doi.org/10.1016/j.idairyj.2016.09.008>
- Jacobs, D. R., & Tapsell, L. C. (2007). Food, not nutrients, is the fundamental unit in nutrition. *Nutrition Reviews*, *65*(10), 439–450.
- Jin, Y., Yu, Y., Qi, Y., Wang, F., Yan, J., & Zou, H. (2016). Peptide profiling and the bioactivity character of yogurt in the simulated gastrointestinal digestion. *Journal of Proteomics*, *141*, 24–46. <https://doi.org/10.1016/j.jprot.2016.04.010>
- Kong, F., & Singh, R. P. (2008). Disintegration of Solid Foods in Human Stomach. *Journal of Food Science*, *73*(5), R67–R80. <https://doi.org/10.1111/j.1750-3841.2008.00766.x>
- Kopec, R. E., Gleize, B., Borel, P., Desmarchelier, C., & Caris-Veyrat, C. (2017). Are lutein, lycopene, and  $\beta$ -carotene lost through the digestive process? *Food & Function*, *8*(4), 1494–1503. <https://doi.org/10.1039/C7FO00021A>
- Lê, S., Josse, J., & Husson, F. (2008). FactoMineR : An R Package for Multivariate Analysis. *Journal of Statistical Software*, *25*(1). <https://doi.org/10.18637/jss.v025.i01>
- Lechevalier, V., Musikaphun, N., Gillard, A., Pasco, M., Guérin-Dubiard, C., Husson, F., & Nau, F. (2015). Effects of dry heating on the progression of in vitro digestion of egg white proteins: contribution of multifactorial data analysis. *Food & Function*, *6*(5), 1578–1590. <https://doi.org/10.1039/C4FO01156B>
- Lorieau, L., Halabi, A., Ligneul, A., Hazart, E., Dupont, D., & Floury, J. (2018). Impact of the dairy product structure and protein nature on the proteolysis and amino acid bioaccessibility during in vitro digestion. *Food Hydrocolloids*, *82*, 399–411. <https://doi.org/10.1016/j.foodhyd.2018.04.019>
- Luo, Q., Boom, R. M., & Janssen, A. E. M. (2015). Digestion of protein and protein gels in simulated gastric environment. *LWT - Food Science and Technology*, *63*(1), 161–168. <https://doi.org/10.1016/j.lwt.2015.03.087>
- Mat, D. J. L., Le Feunteun, S., Michon, C., & Souchon, I. (2016). In vitro digestion of foods using pH-stat and the INFOGEST protocol: Impact of matrix structure on digestion kinetics of macronutrients, proteins and lipids. *Food Research International*, *88*, 226–233. <https://doi.org/10.1016/j.foodres.2015.12.002>
- Miller, L. & Houghton, J. The Micro-Kjeldahl Determination of the Nitrogen Content of Amino Acids and Proteins. *The Journal of Biological Chemistry*. Mars 1945, n°159, p. 373-383.
- Minekus, M., Alming, M., Alvito, P., Ballance, S., Bohn, T., Bourlieu, C., Carrière, F., Boutrou, R., Corredig, M., Dupont, D., Dufour, C., Egger, L., Golding, M., Karakaya, S., Kirkhus, B., Le Feunteun, S., Lesmes, U., Macierzanka, A., Mackie, A., Marze, S., McClements, DJ., Ménard, O., Recio, I.,

- Santos, CN., Singh, RP., Vegarud, GE., Wickham, MS., Weitschies, W., Brodtkorb, A. (2014). A standardised static in vitro digestion method suitable for food – an international consensus. *Food & Function*, 5(6), 1113. <https://doi.org/10.1039/c3fo60702j>
- Moorhead, S. A., Welch, R. W., Barbara, M., Livingstone, E., McCourt, M., Burns, A. A., & Dunne, A. (2006). The effects of the fibre content and physical structure of carrots on satiety and subsequent intakes when eaten as part of a mixed meal. *The British Journal of Nutrition*, 96(3), 587–595.
- Morell, P., Fizman, S., Llorca, E., & Hernando, I. (2017). Designing added-protein yogurts: Relationship between in vitro digestion behavior and structure. *Food Hydrocolloids*, 72, 27–34. <https://doi.org/10.1016/j.foodhyd.2017.05.026>
- Mulet-Cabero, A.-I., Rigby, N. M., Brodtkorb, A., & Mackie, A. R. (2017). Dairy food structures influence the rates of nutrient digestion through different in vitro gastric behaviour. *Food Hydrocolloids*, 67, 63–73. <https://doi.org/10.1016/j.foodhyd.2016.12.039>
- Nielsen, J. E., Borchert, T. V., & Vriend, G. (2001). The determinants of  $\alpha$ -amylase pH-activity profiles. *Protein Engineering, Design and Selection*, 14(7), 505–512. <https://doi.org/10.1093/protein/14.7.505>
- Nyemb, K., Guérin-Dubiard, C., Pézennec, S., Jardin, J., Briard-Bion, V., Cauty, C., Dupont, D., Nau, F. (2016). The structural properties of egg white gels impact the extent of in vitro protein digestion and the nature of peptides generated. *Food Hydrocolloids*, 54, 315–327. <https://doi.org/10.1016/j.foodhyd.2015.10.011>
- Nyemb-Diop, K., Causeur, D., Jardin, J., Briard-Bion, V., Guérin-Dubiard, C., Rutherford, S. M., Dupont, D., Nau, F. (2016). Investigating the impact of egg white gel structure on peptide kinetics profile during in vitro digestion. *Food Research International*, 88, 302–309. <https://doi.org/10.1016/j.foodres.2016.01.004>
- Peyron, M.-A., Mishellany, A., & Woda, A. (2004). Particle size distribution of food boluses after mastication of six natural foods. *Journal of Dental Research*, 83(7), 578–582.
- R Development Core Team (2007) R: A Language and Environment for Statistical Computing. R Foundation for Statistical Computing, Vienna. <http://www.R-project.org>
- Reboul, E., Richelle, M., Perrot, E., Desmoulins-Malezet, C., Pirisi, V., & Borel, P. (2006). Bioaccessibility of Carotenoids and Vitamin E from Their Main Dietary Sources. *Journal of Agricultural and Food Chemistry*, 54(23), 8749–8755. <https://doi.org/10.1021/jf061818s>
- Rinaldi, L., Gauthier, S. F., Britten, M., & Turgeon, S. L. (2014). In vitro gastrointestinal digestion of liquid and semi-liquid dairy matrixes. *LWT - Food Science and Technology*, 57(1), 99–105. <https://doi.org/10.1016/j.lwt.2014.01.026>

- Ristow, K. A., Gregory, J. F., & Damron, B. L. (1982). Effects of dietary fiber on the bioavailability of folic acid monoglutamate. *The Journal of Nutrition*, *112*(4), 750–758. <https://doi.org/10.1093/jn/112.4.750>
- Seligman, S., Copeland, L., Appels, R., & Morell, M. (1998). Analysis of lipids binding to starch. In *Cereals* (pp. 87–90). Australia, North Melbourne: Royal Australian Chemical Institute.
- Singh, J., Dartois, A., & Kaur, L. (2010). Starch digestibility in food matrix: a review. *Trends in Food Science & Technology*, *21*(4), 168–180. <https://doi.org/10.1016/j.tifs.2009.12.001>
- Singh, J., Kaur, L., & Singh, H. (2013). Food Microstructure and Starch Digestion. In *Advances in Food and Nutrition Research* (Vol. 70, pp. 137–179). <https://doi.org/10.1016/B978-0-12-416555-7.00004-7>
- Tamura, M., Singh, J., Kaur, L., & Ogawa, Y. (2016). Impact of the degree of cooking on starch digestibility of rice – An in vitro study. *Food Chemistry*, *191*, 98–104. <https://doi.org/10.1016/j.foodchem.2015.03.127>
- Tyssandier, V., Reboul, E., Dumas, J.-F., Bouteloup-Demange, C., Armand, M., Marcand, J., Sallas, M., Borel, P. (2003). Processing of vegetable-borne carotenoids in the human stomach and duodenum. *American Journal of Physiology-Gastrointestinal and Liver Physiology*, *284*(6), G913–G923. <https://doi.org/10.1152/ajpgi.00410.2002>
- van het Hof, K., Tijburg, L., Pietrzik, K., & Weststrate, J. (1999). *Influence of feeding different vegetables on plasma levels of carotenoids, folate and vitamin C. Effect of disruption of the vegetable matrix.* *3*(82), 203–212.
- Wu, Z., Li, X., Hou, C., & Qian, Y. (2010). Solubility of Folic Acid in Water at pH Values between 0 and 7 at Temperatures (298.15, 303.15, and 313.15) K. *Journal of Chemical & Engineering Data*, *55*(9), 3958–3961. <https://doi.org/10.1021/jc1000268>



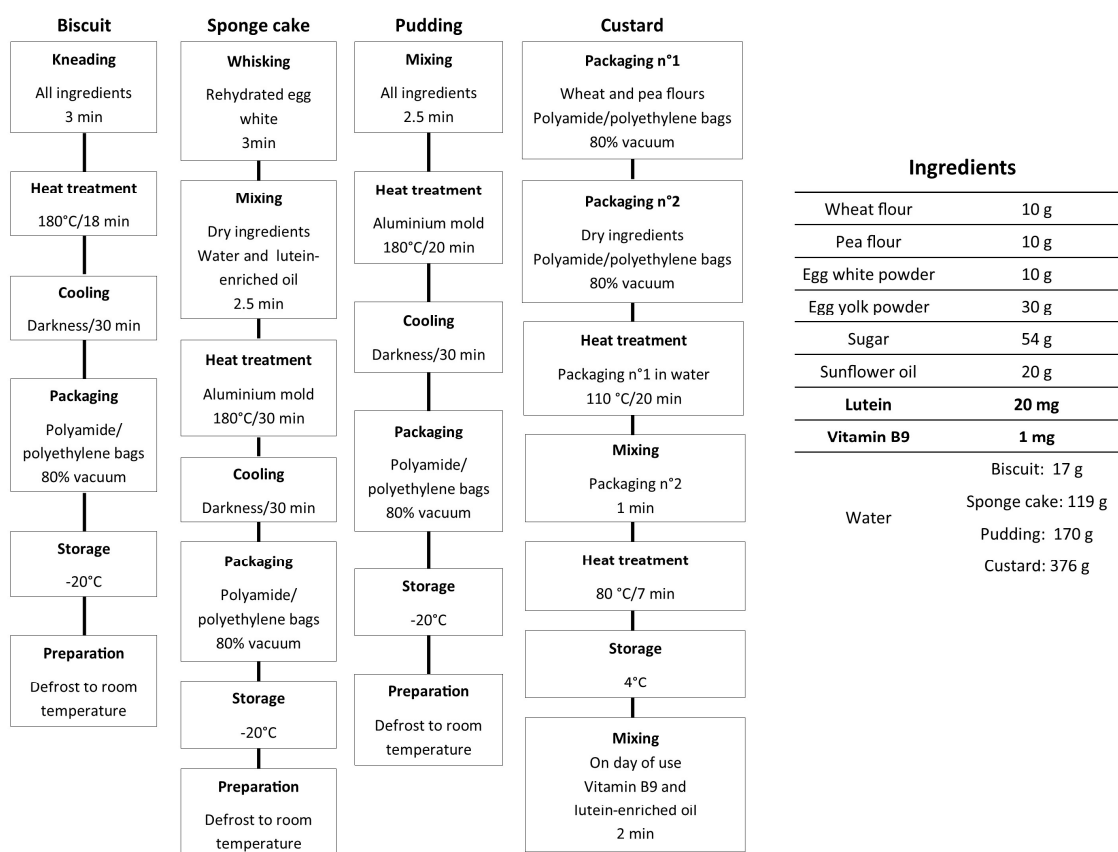


Figure 1. Production flowcharts and food composition.



Figure 2. Macroscopic images of the four foods: Biscuit, Sponge cake, Pudding and Custard (from left to right).

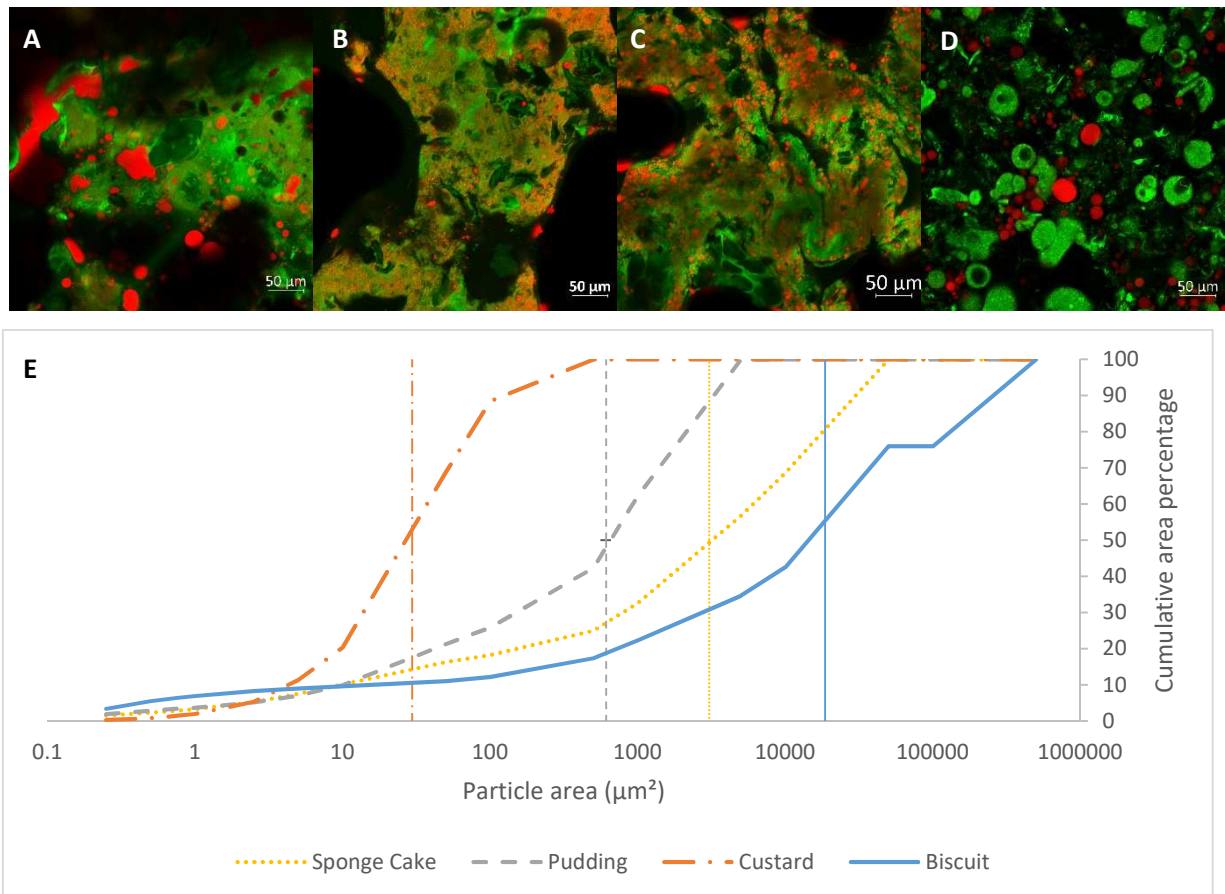


Figure 3. Confocal images of the Biscuit (A), Sponge cake (B), Pudding (C), and Custard (D) at a magnification of x20 (lipids appear in red and proteins in green), and size distribution of lipid droplets in the four foods represented by their cumulative area percentage (E: vertical lines correspond to  $x_{50}$ , the median of each distribution).

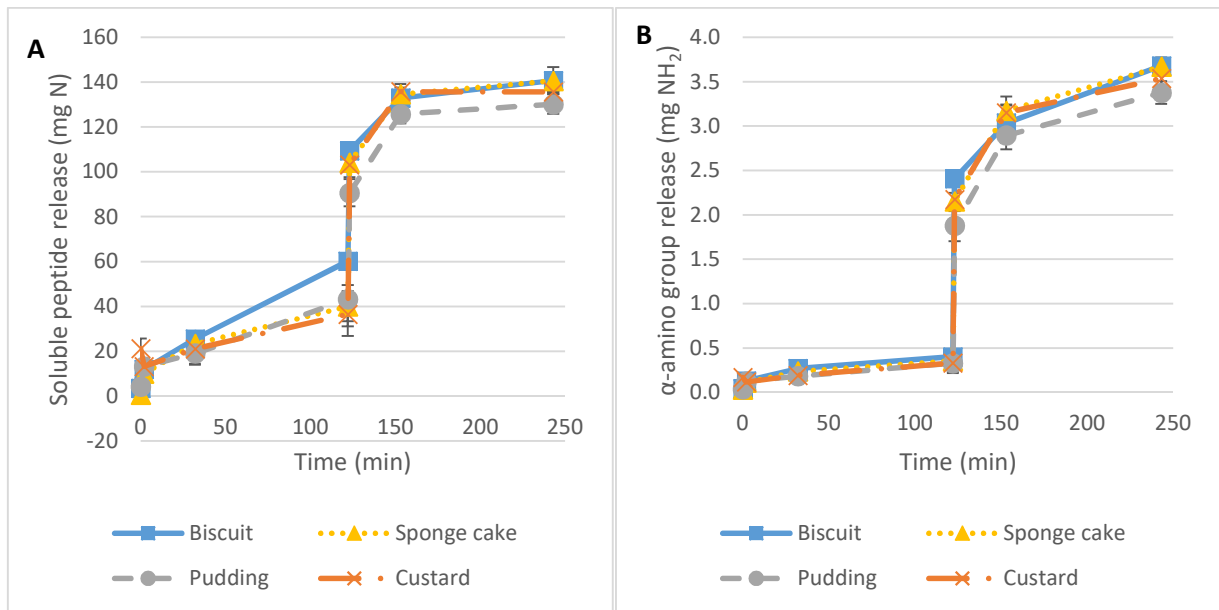


Figure 4. Protein digestion: Peptide release (a) and free amino group release (b) during *in vitro* digestion of the four foods.

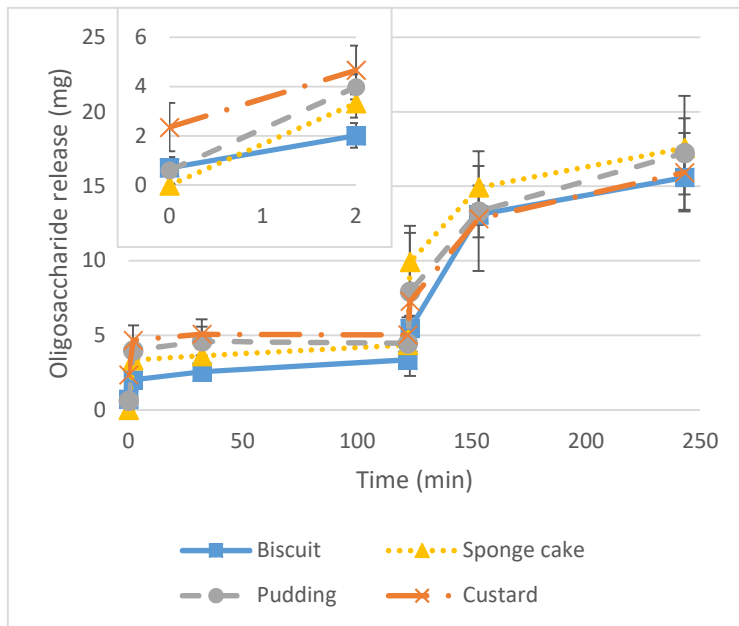


Figure 5. Carbohydrate digestion: Release of oligosaccharides during *in vitro* digestion of the four foods; top left insert is a zoom on the oral phase.

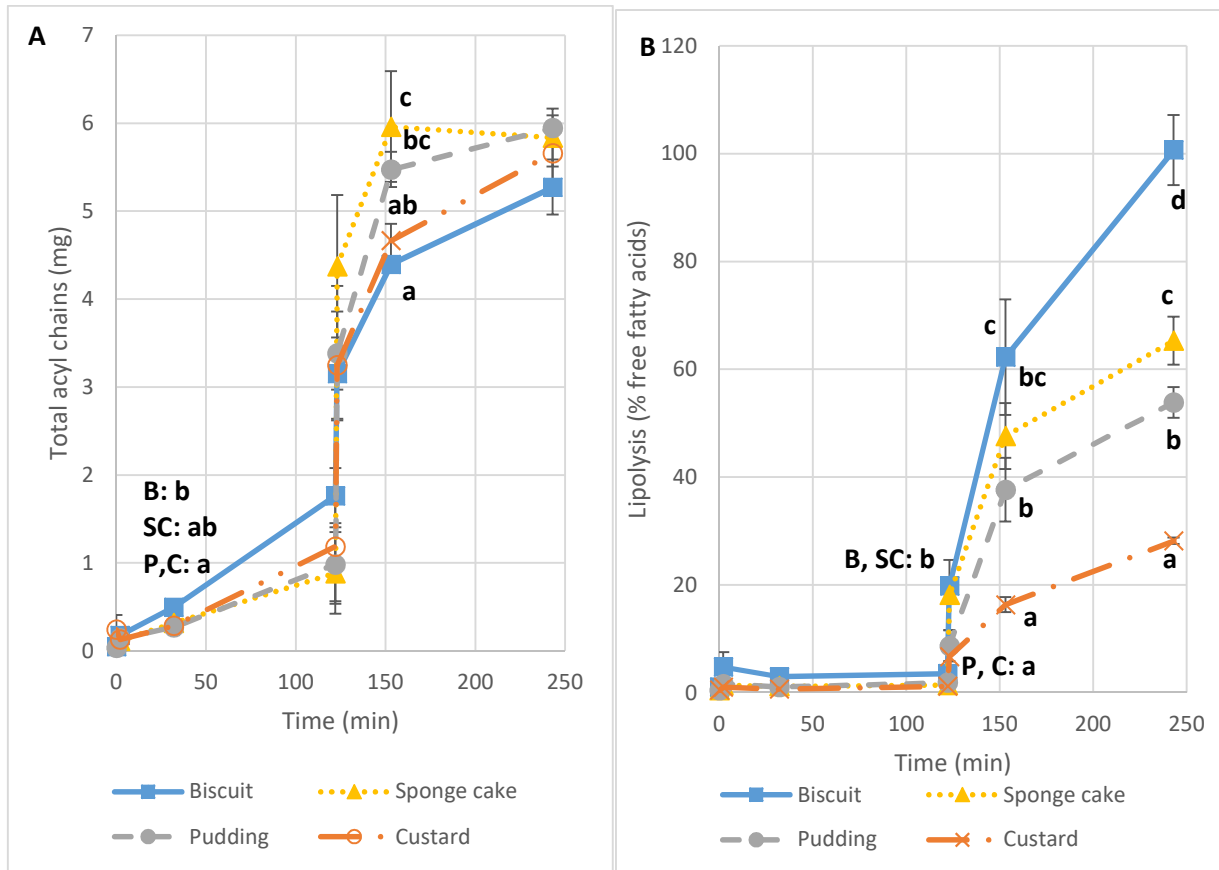


Figure 6. Lipid digestion: Lipid release (A) and lipolysis (B) during *in vitro* digestion of the four foods. At a given time, the differences between matrices are demonstrated by different letters ( $P < 0.05$ ).

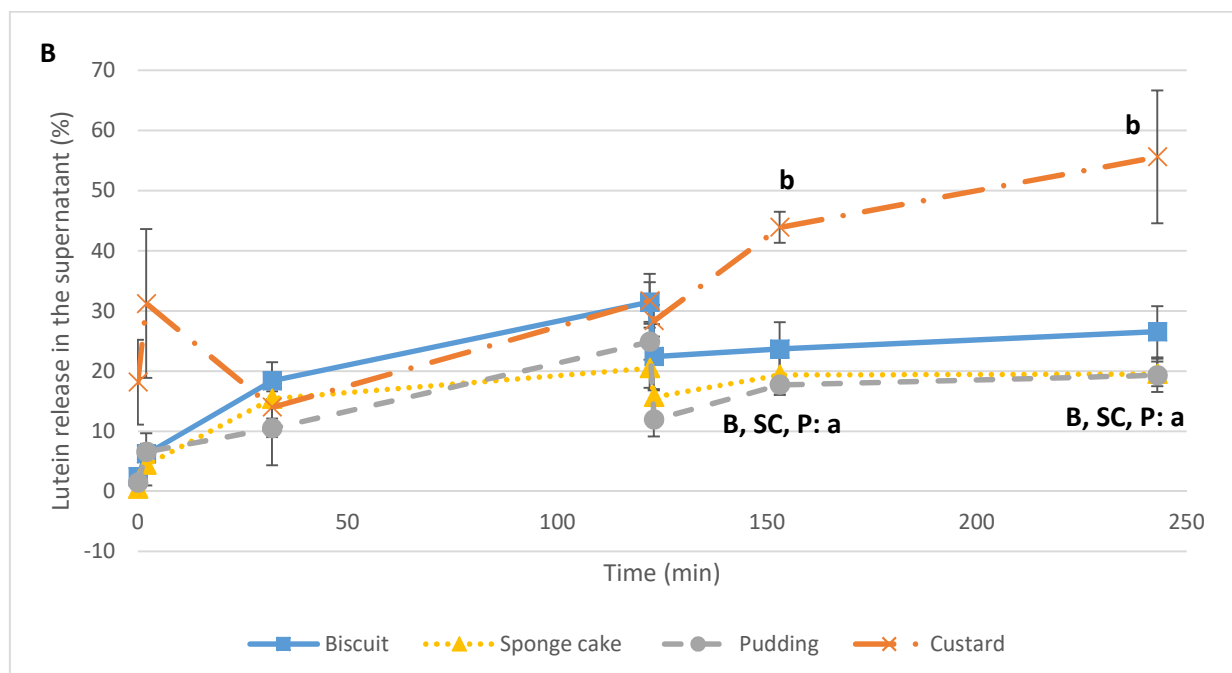
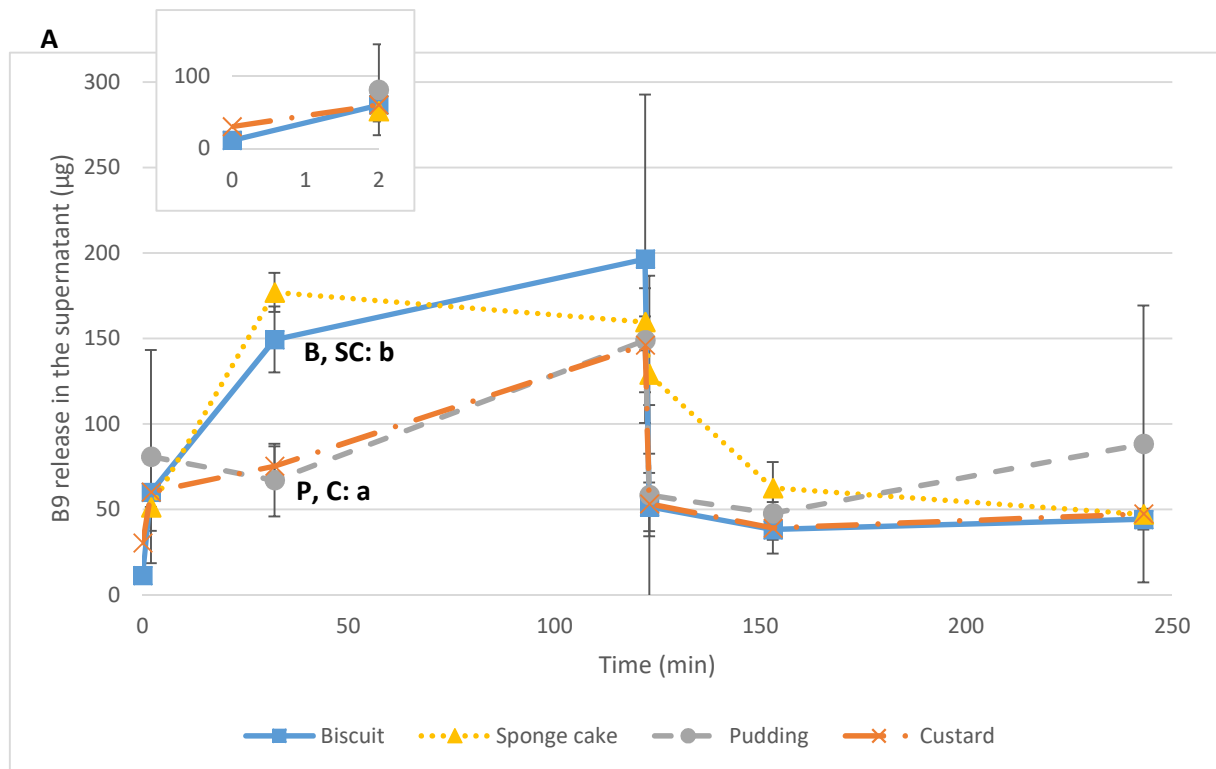


Figure 7. Micronutrient bioaccessibility: vitamin B9 (A) and lutein (B) release in the supernatant during *in vitro* digestion of the four foods. Lutein release is expressed as the percentage of the total amount quantified at each digestion time to account for the progressive degradation of lutein under *in vitro* digestion conditions. Top left insert (A) is a zoom on the oral phase.

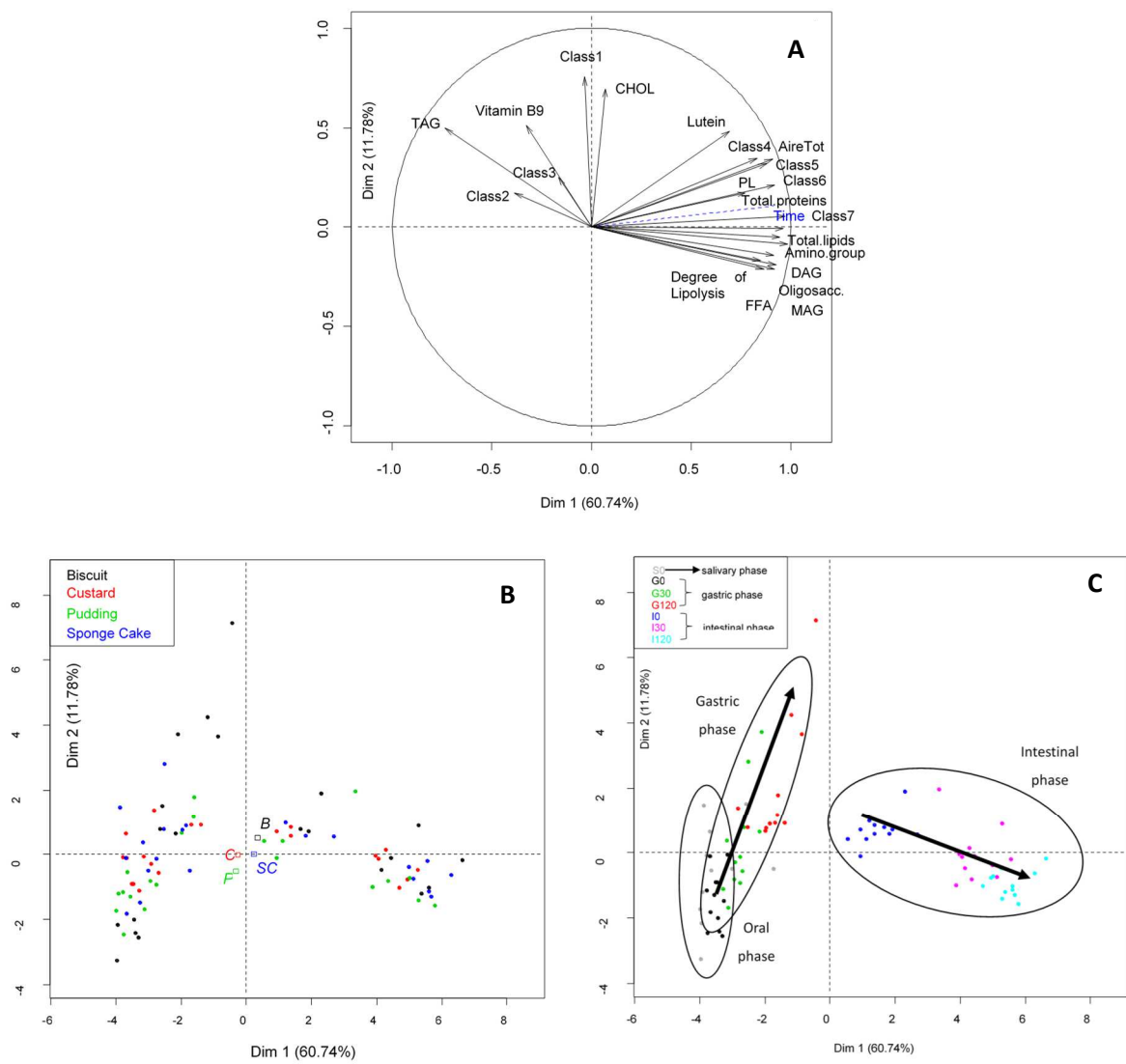


Figure 8. Projection of the variables (A) and of the individuals (B, C) on the first two dimensions (PC1 and PC2) of the principal component analysis (PCA). (A) Active variables (in black) correspond to the characteristics measured on the *in vitro* digesta. Digestion time was added as an illustrative variable (in blue). Individuals are identified according to the food matrix (B) or to the digestion time (C). (B) Empty squares correspond to the barycentre of each of the four foods. (C) Black arrows represent the direction of the digestion process during the gastric and intestinal phases.



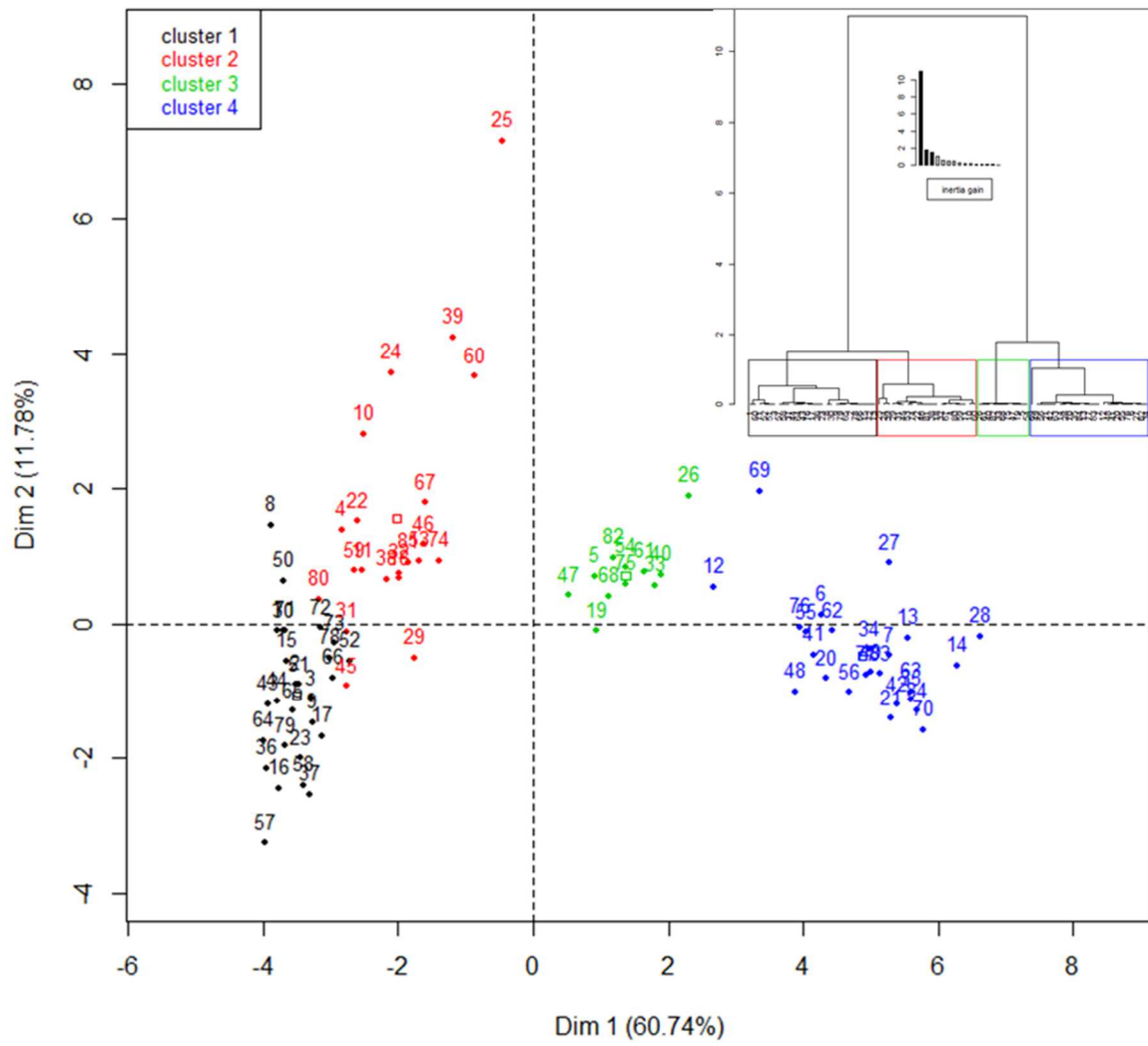


Figure 9. Hierarchical clustering analysis (HCA) applied to the first two principal components of the PCA.

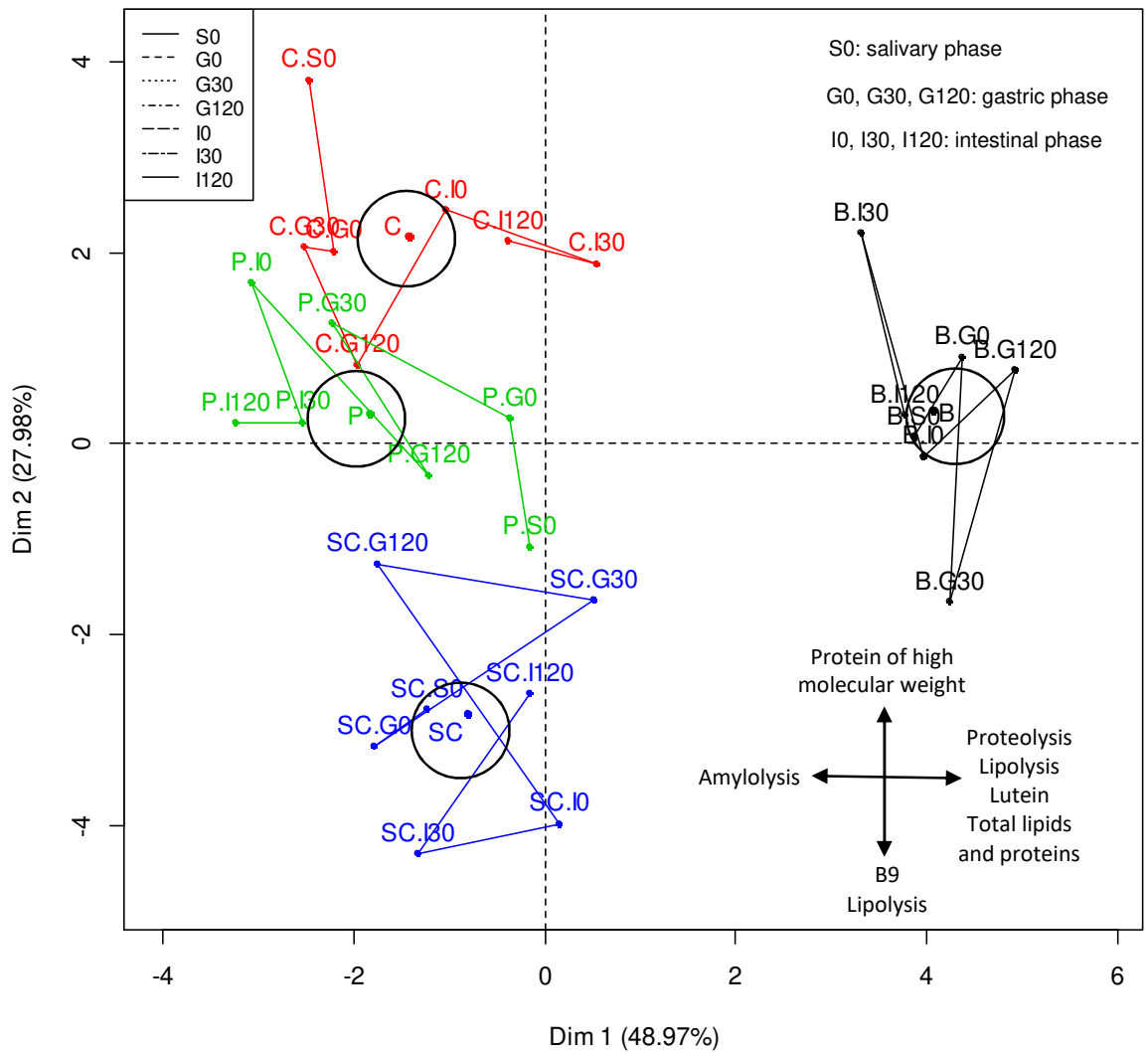


Figure 10. MFA map of the individuals for the four foods during *in vitro* digestion. Lines illustrate the changes of the individuals' coordinates throughout digestion; circles indicate the barycentres for each food.

Table 1. Details and meaning of variables obtained from supernatant analysis.

Nutrients	Variables	Analysis performed	Result expressed (and meaning)
Micronutrients	Vitamin B9	Reverse phase HPLC	Quantity of vitamin B9 released in the supernatant (bioaccessibility)
	Lutein	Reverse phase HPLC	Ratio of lutein released in the supernatant/total lutein (bioaccessibility)
Carbohydrates	Oligosacc.	UV-visible absorbance	Quantification of oligosaccharides released in the supernatant (degree of amylolysis)
Lipids	Total lipids	UV-visible absorbance	Quantification of total acyl chains solubilised in the supernatant (food disintegration)
	Degree of lipolysis	Gas chromatography	Ratio of free fatty acids released in the supernatant/total fatty acids (degree of lipolysis)
	TAG, FFA, DAG, MAG, PL, CHOL	Thin layer chromatography	Relative content of each lipid class (lipolysis kinetics)
Proteins	Total nitrogen	Kjeldahl quantification	Total quantity of nitrogen solubilised in the supernatant (food disintegration)
	AminoGroup	OPA quantification	Free amino group release in the supernatant (degree of proteolysis)
	Classes 1 to 7	Size Exclusion Chromatography	Quantity of peptides in each size class released in the supernatant (size distribution of peptides)
	AireTot	Size Exclusion Chromatography	Total quantity of peptides in the supernatant (degree of proteolysis)

Table 2. Statistical significance of the variables “Food matrix” and “Digestion time” on the characteristics of *in vitro* digesta, model R<sup>2</sup> and the p-value of the linear model.

	Matrix	Time	Matrix * Time	R <sup>2</sup>	p-value
Lutein	***	***	***	0.844	2.10 <sup>-16</sup>
Vitamin B9	NS	***	NS	0.505	4.10 <sup>-5</sup>
Oligosacc.	*	***	NS	0.900	2.10 <sup>-16</sup>
Total lipids	**	***	***	0.974	2.10 <sup>-16</sup>
Degree of Lipolysis	***	***	***	0.983	2.10 <sup>-16</sup>
TAG	*	***	**	0.730	1.10 <sup>-12</sup>
FFA	**	***	**	0.980	2.10 <sup>-16</sup>
DAG	*	***	**	0.979	2.10 <sup>-16</sup>
MAG	**	***	*	0.914	2.10 <sup>-16</sup>
CHOL	*	NS	NS	0.174	0.058
PL	***	***	*	0.810	2.10 <sup>-16</sup>
Total proteins	**	***	*	0.982	2.10 <sup>-16</sup>
AminoGroup	***	***	**	0.996	2.10 <sup>-16</sup>
Class1	***	***	NS	0.437	7.10 <sup>-5</sup>
Class2	***	***	***	0.618	1.10 <sup>-8</sup>
Class3	**	NS	NS	0.237	0.019
Class4	***	***	NS	0.934	2.10 <sup>-16</sup>
Class5	**	***	NS	0.881	2.10 <sup>-16</sup>
Class6	***	***	NS	0.891	2.10 <sup>-16</sup>
Class7	**	***	NS	0.918	2.10 <sup>-16</sup>
AireTot	***	***	NS	0.890	2.10 <sup>-16</sup>

\* Significant effect at p < 0.05; \*\* significant effect at p < 0.01; \*\*\* significant effect at p < 0.001; NS, no significant effect. Variable meanings are indicated in Table 1.



**In Vitro Digestion Method for Food**

